

Formation of highly excited iodine atoms from multiphoton excitation of CH₃I

Kristján Matthíasson^{1#}, Greta Koumarianou^{2#}, Meng-Xu Jiang^{1#}, Pavle Glodic^{2#}
Peter C. Samartzis^{2*} and Águst Kvaran^{1*}

1. *Science Institute, University of Iceland, Dunhagi 3, 107 Reykjavík, Iceland.*
2. *Institute of Electronic Structure and Laser, Foundation for Research and Technology-Hellas, Vassilika Vouton, 71110 Heraklion, Greece.*

Supplementary material

Content:	pages:
Fig. S1: I ⁺ ion REMPI Spectra.....	1
Fig. S2: Non-resonance mass spectra at 69 384 cm ⁻¹ and 69 539 cm ⁻¹	2
Fig. S3 (a – c): Photoelectron KERs.....	3 – 5
Fig. S4 (a - h): Angular distributions for CH ₃ ⁺ images.....	6 – 9
Fig. S5 (a - h): Angular distributions for I ⁺ images.....	10 – 13
Table S1: Anisotropy parameters for CH ₃ ⁺ images	14
Table S2: Anisotropy parameters for I ⁺ images	15

Fig. S1

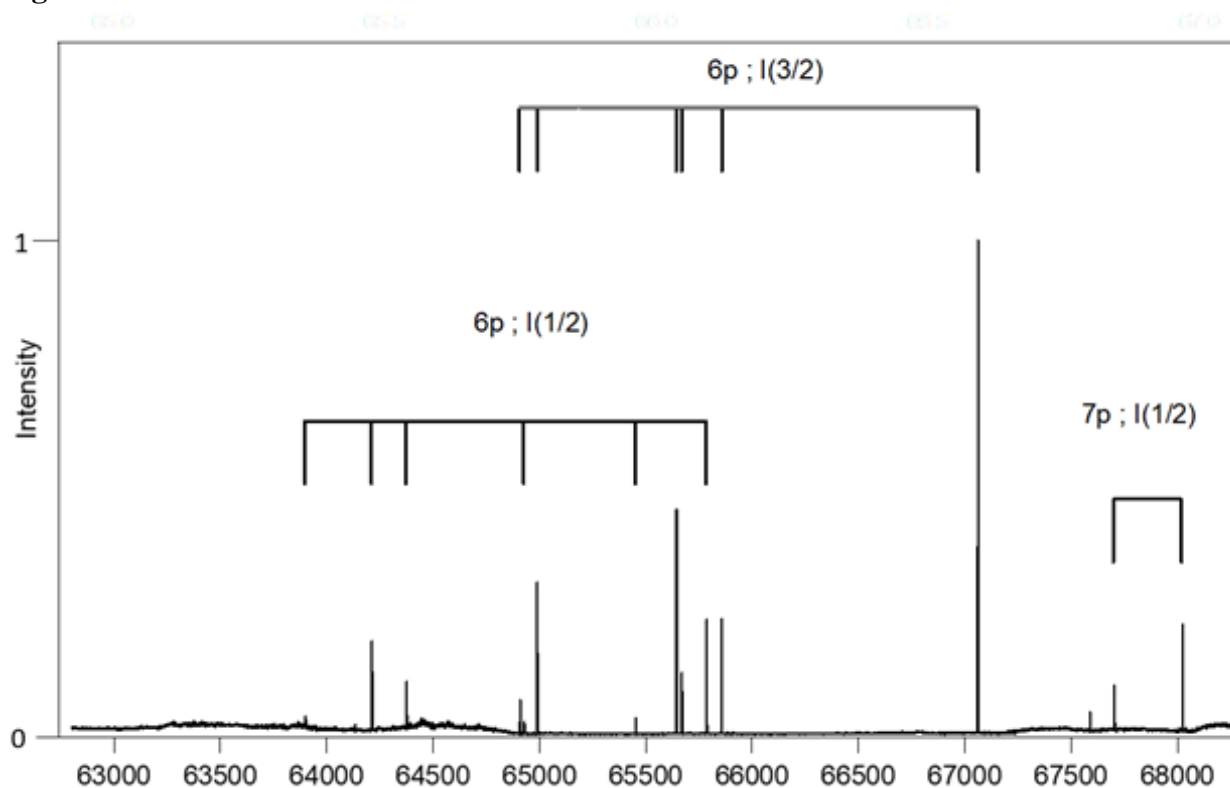


Fig. S1: Figure shows REMPI spectra for I^+ ion in the energy region of $65\ 000\ \text{cm}^{-1}$ to $70\ 000\ \text{cm}^{-1}$. Grid shows iodine atomic lines according to NIST. Atomic lines originate from either iodine atoms in the ground ($I(3/2)$) or the spin-orbit excited ($I(1/2)$) state.

Fig. S2

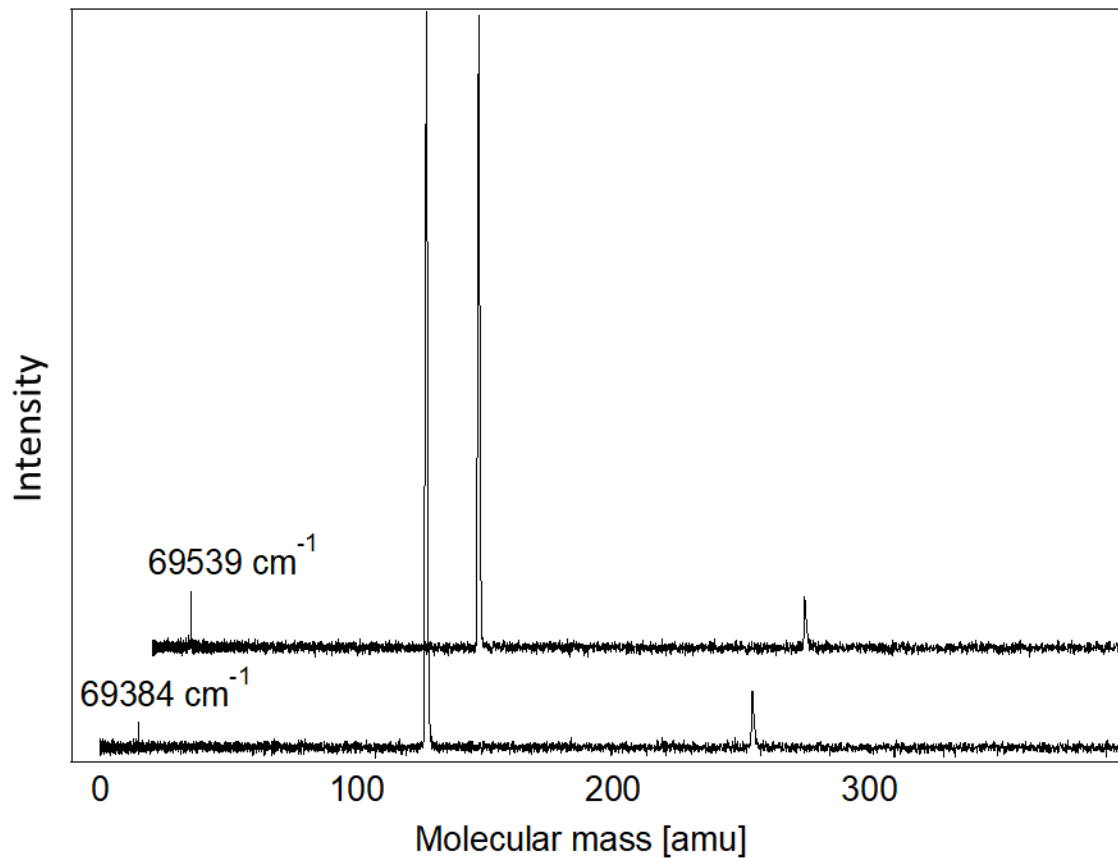


Fig. S2: Figure shows mass spectra at non-resonant frequencies of $69\ 384\text{ cm}^{-1}$ and $69\ 539\text{ cm}^{-1}$. CH_3^+ , I^+ and I_2^+ mass peaks are observed due to non-resonance excitation and ionization.

Fig. S3

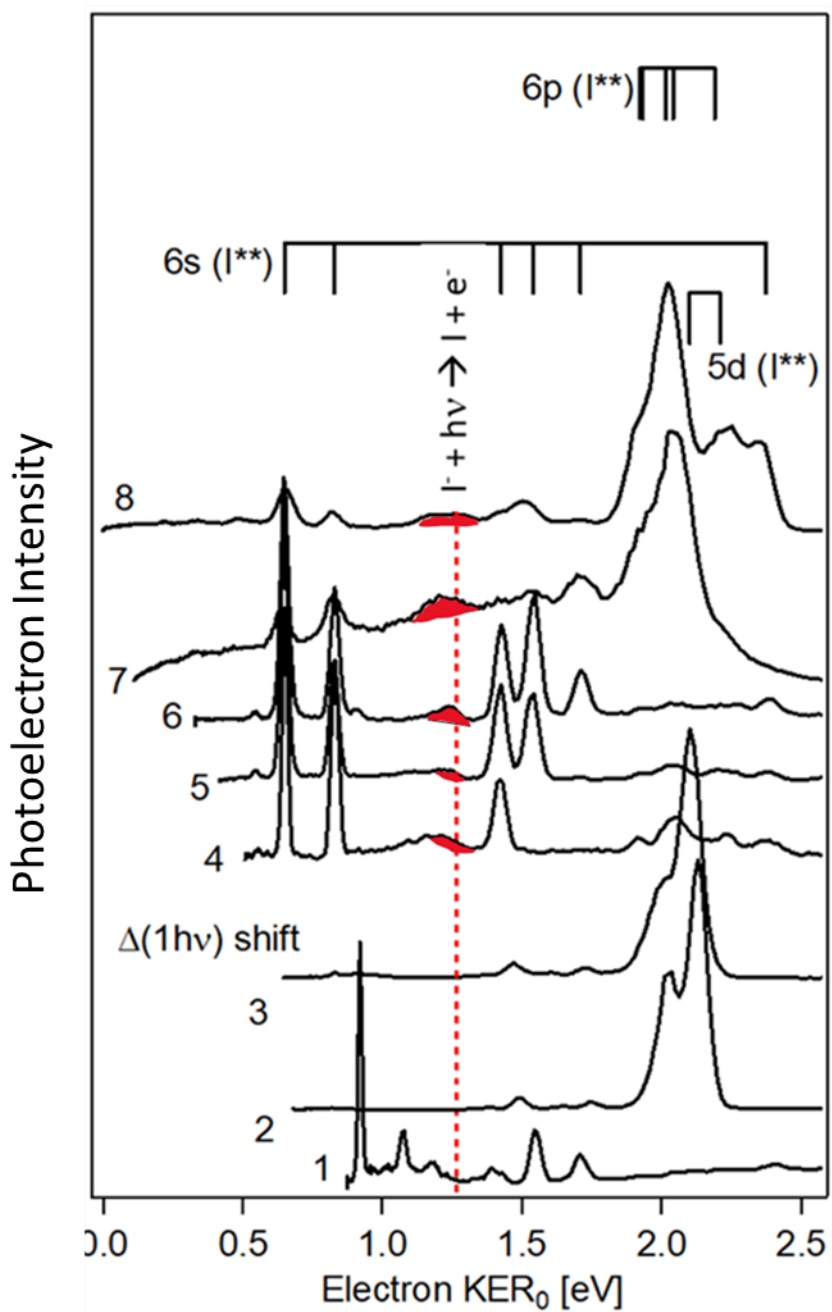


Fig. S3a: Photoelectron KERs derived from images no. 1 – 8 (see paper main text) shifted by a one-photon energy difference ($\Delta(1h\nu) = |1h\nu_i - 1h\nu_0|$) with respect to the spectrum for the highest energy excitation (i.e. reference spectrum, no. 8). Common energy thresholds (energy maxima) for one-photon ionization of Rydberg iodine atoms (I^{**}) are indicated by sticks above the KERs. The threshold for electron ejection of I is indicated by a red broken line and the corresponding peaks(shoulders) are highlighted in red. The spectra are normalized to the strongest peak in each spectrum.

Fig. S3

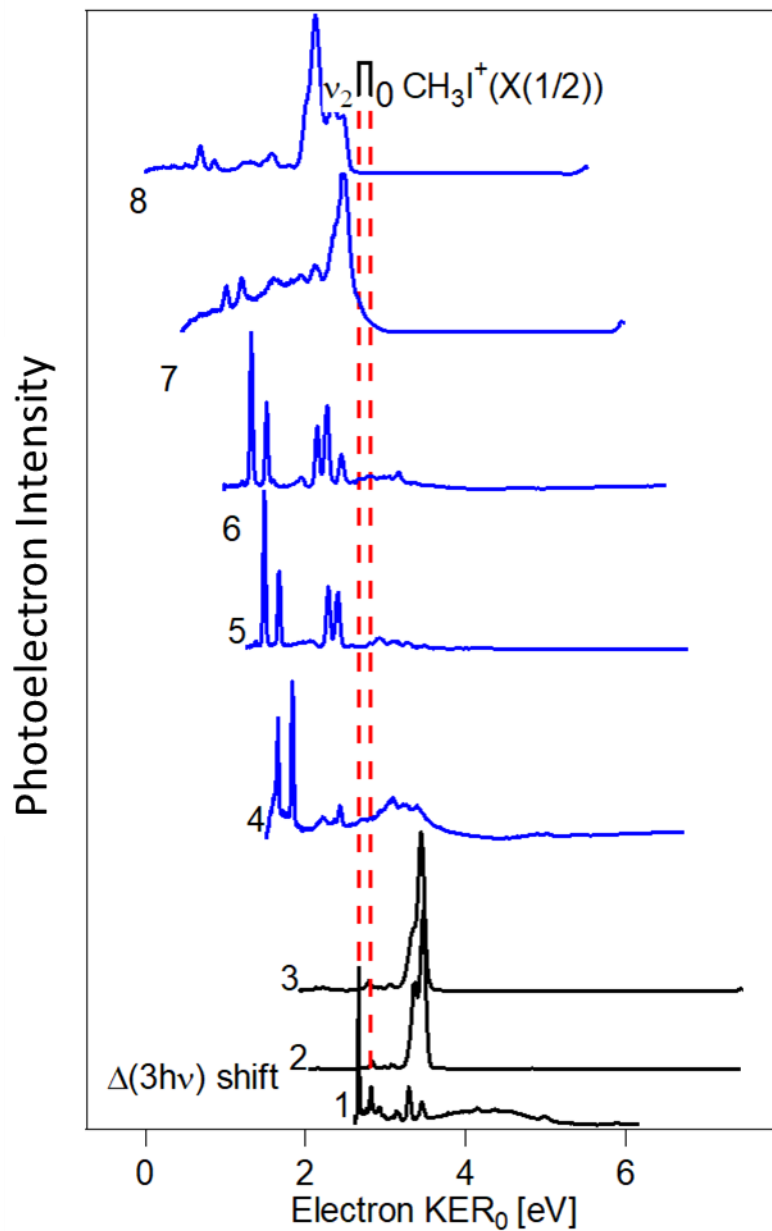


Fig. S3b: Photoelectron KERs derived from images 1 – 8 (see paper main text) shifted by a three-photon energy difference ($\Delta(3h\nu) = \beta h\nu_i - 3h\nu_0$) with respect to the spectrum for the highest energy excitation (i.e. reference spectrum, no. 8). Common energy thresholds (energy maxima) for autoionization of superexcited CH_3I ($\text{CH}_3\text{I}^\#$) are indicated by sticks above the KERs. The spectra are plotted as a function of the electron KER for the reference spectra (KER₀). The spectra are normalized to the strongest peak in each spectrum.

Fig. S3

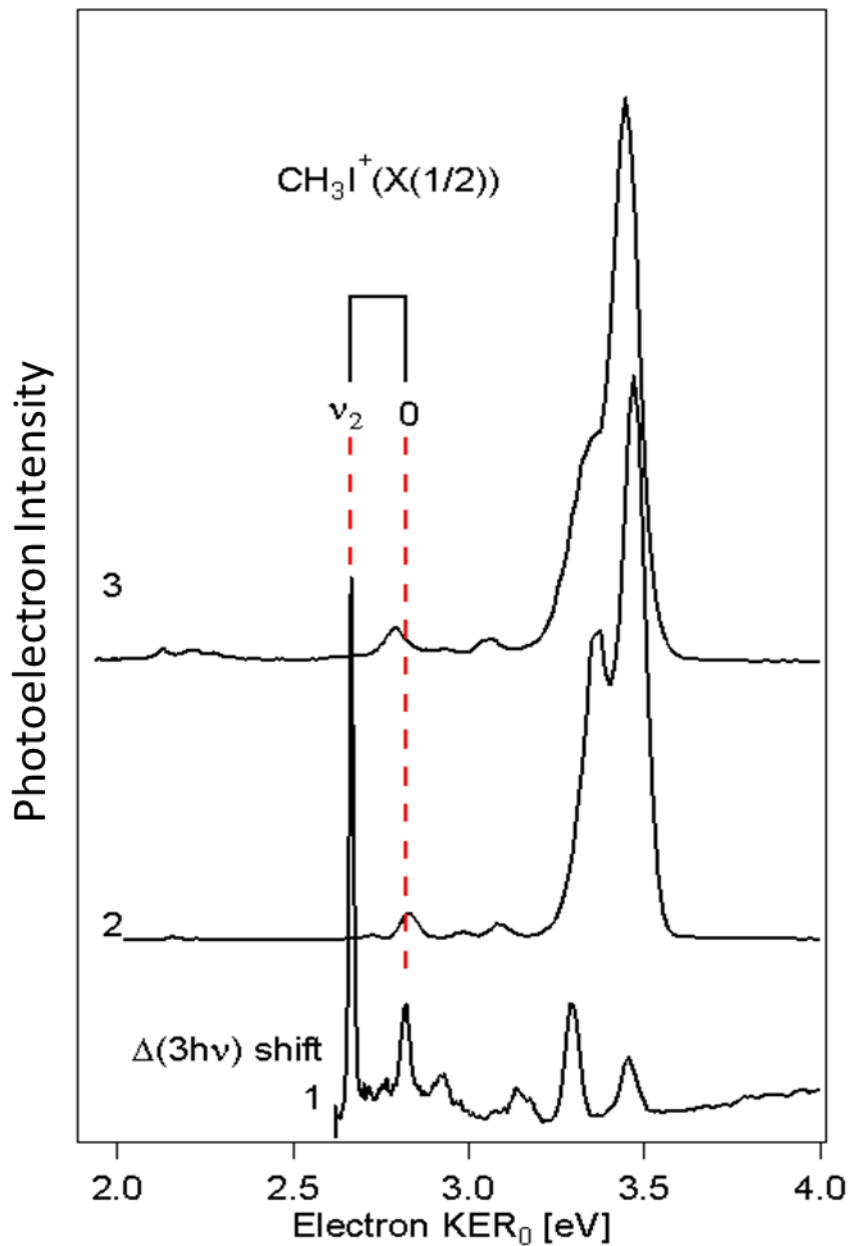


Fig. S3c: Photoelectron KERs derived from images 1 – 3 (see paper main text) shifted by a three-photon energy difference ($\Delta(3h\nu) = \beta h\nu_i - 3h\nu_0$) with respect to the spectrum for the highest energy excitation recorded (i.e. reference spectrum, no. 8). Common energy thresholds (energy maxima) for autoionization of superexcited CH_3I ($\text{CH}_3\text{I}^\#$) are indicated by sticks above the KERs. The spectra are plotted as a function of the electron KER for the reference spectra (KER₀). The spectra are normalized to the strongest peak in each spectrum.

Fig. S4.

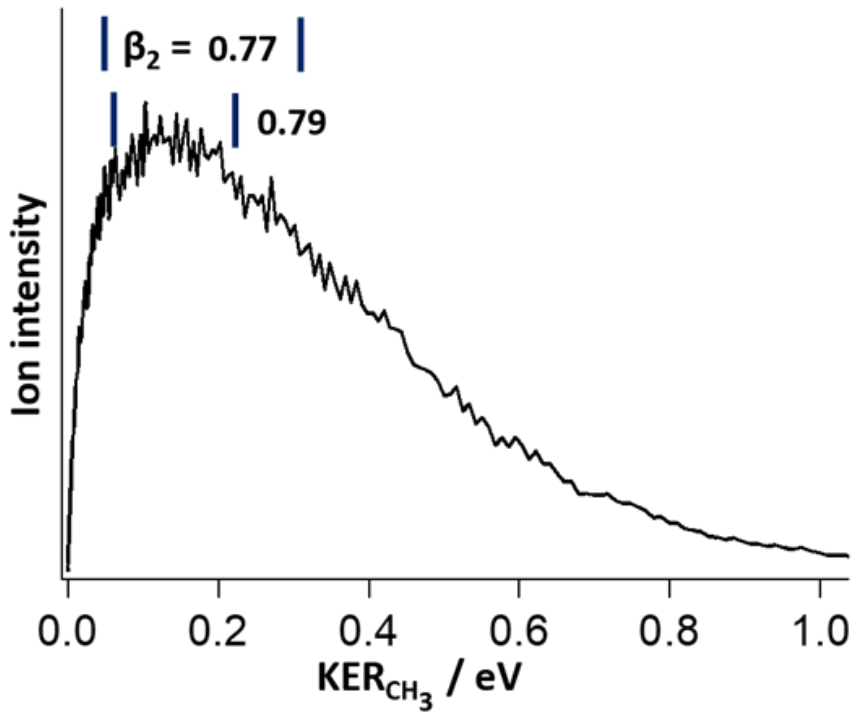


Fig. S4-a: CH_3^+ KER spectrum and anisotropy, β_2 values. $2hv = 55700 \text{ cm}^{-1}$.

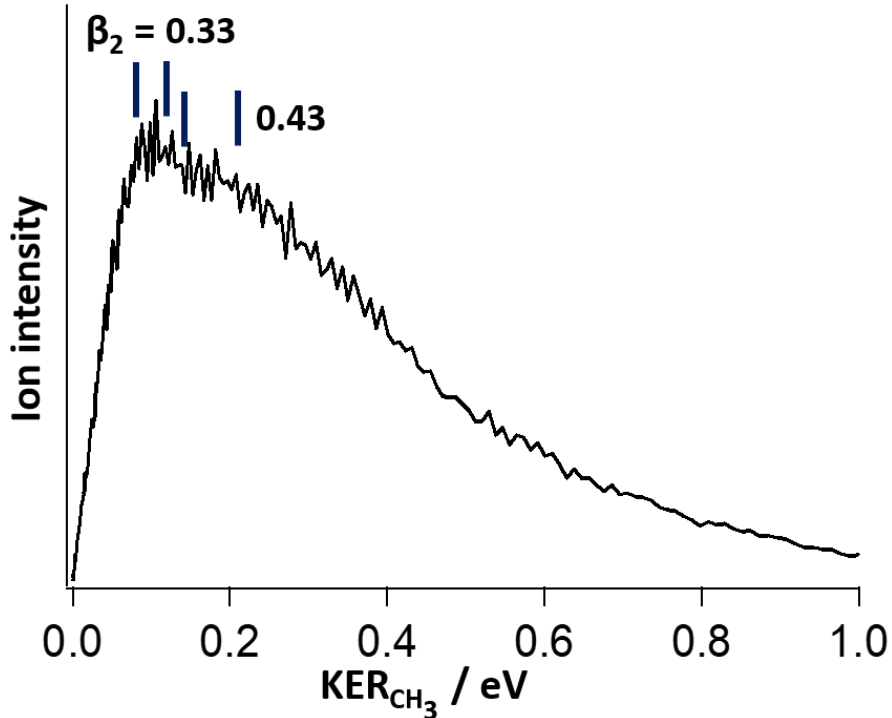


Fig. S4-b: CH_3^+ KER spectrum and anisotropy, β_2 values. $2hv = 58926 \text{ cm}^{-1}$.

Fig. S4.

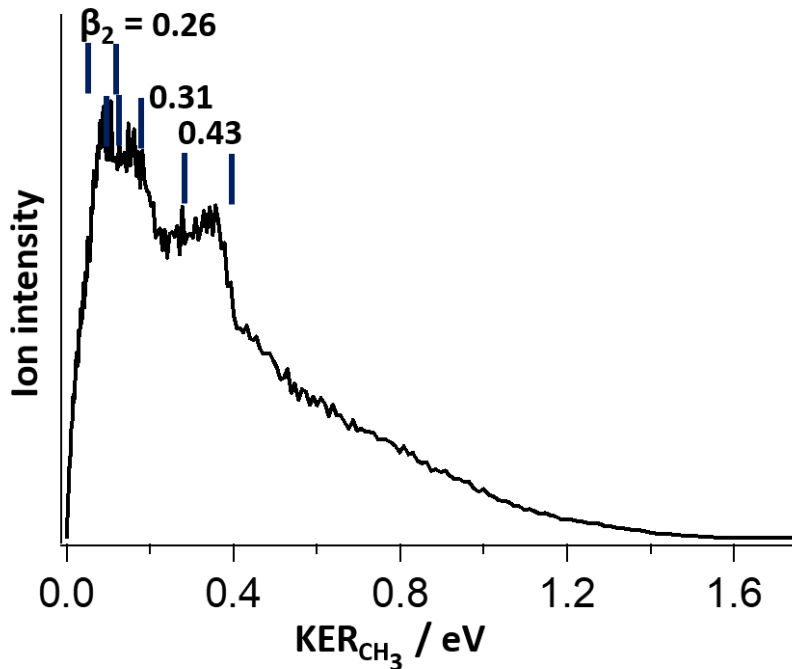


Fig. S4-c: CH_3^+ KER spectrum and anisotropy, β_2 values. $2hv = 59362\text{ cm}^{-1}$.

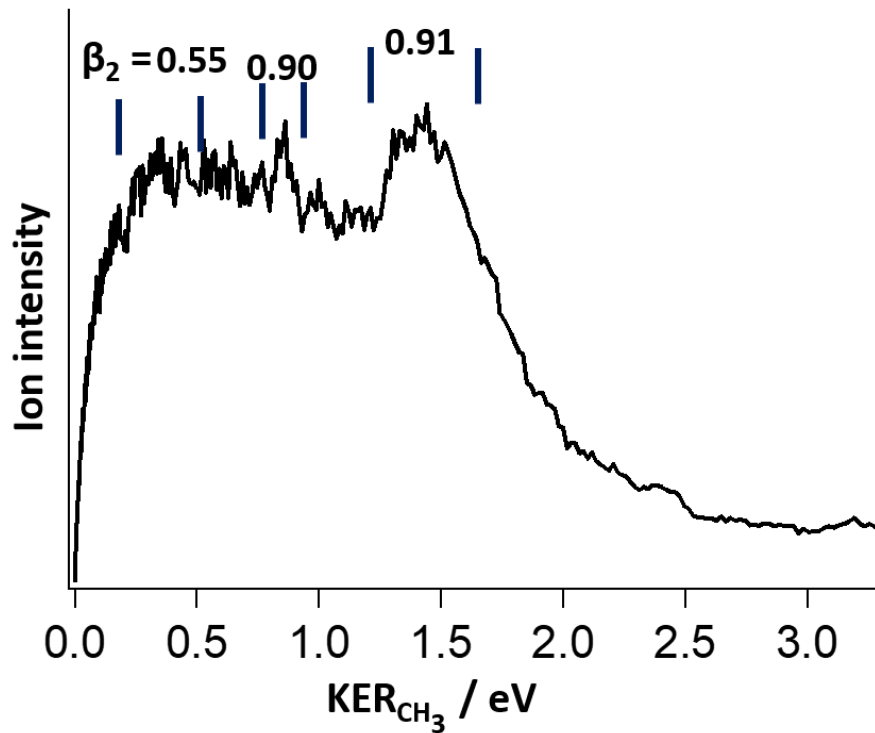


Fig. S4-d: CH_3^+ KER spectrum and anisotropy, β_2 values. $2hv = 61632\text{ cm}^{-1}$.

Fig. S4.

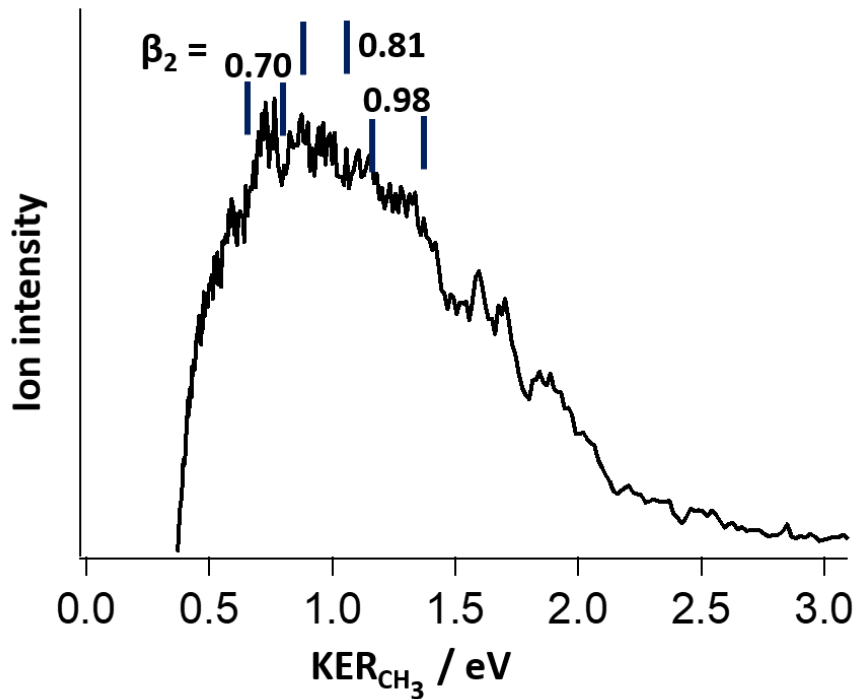


Fig. S4-e: CH_3^+ KER spectrum and anisotropy, β_2 values. $2hv = 63067 \text{ cm}^{-1}$.

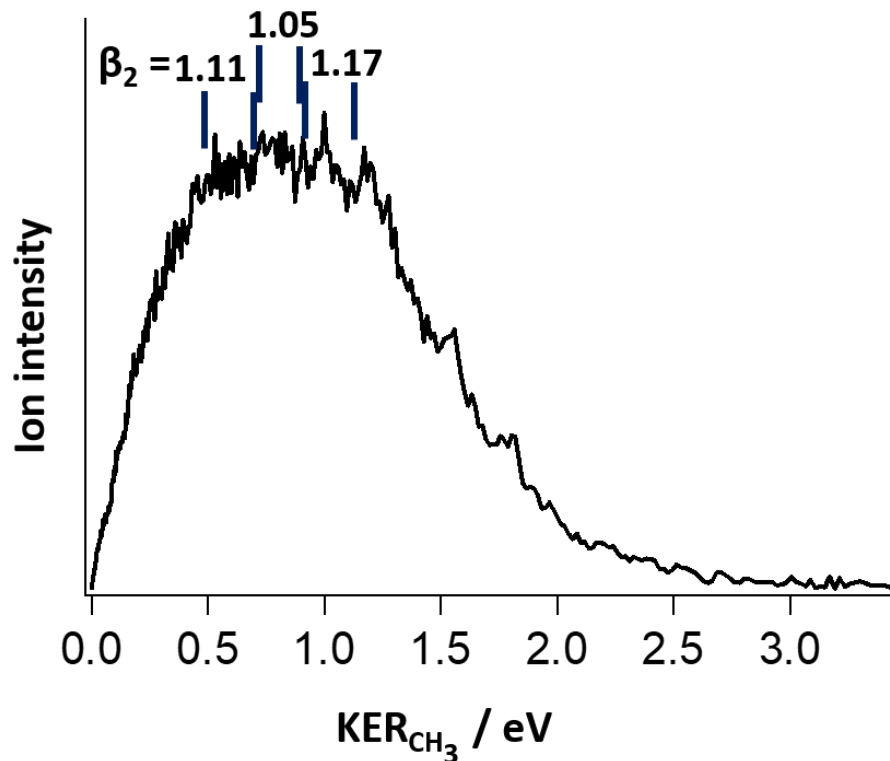


Fig. S4-f: CH_3^+ KER spectrum and anisotropy, β_2 values. $2hv = 64484 \text{ cm}^{-1}$.

Fig. S4.

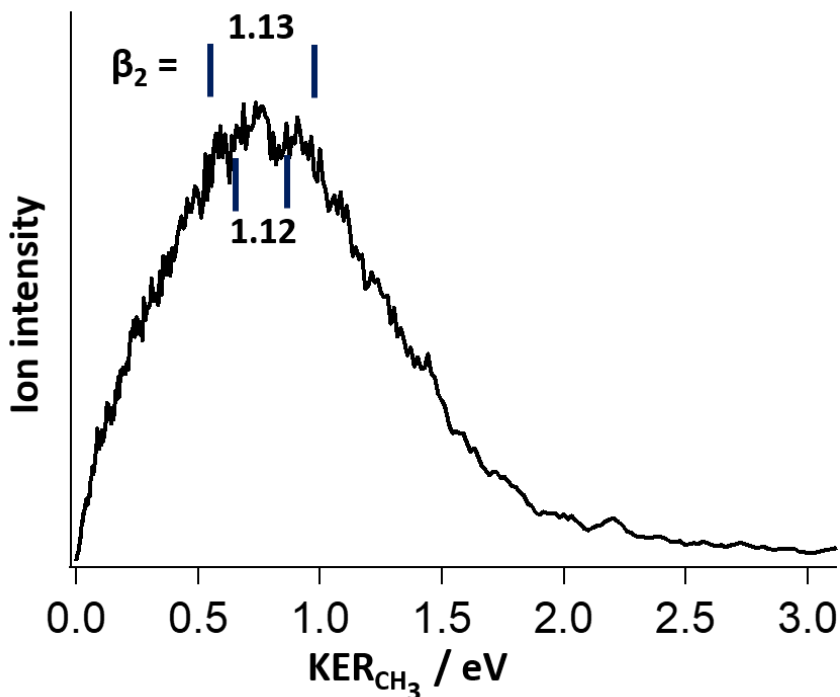


Fig. S4-g: CH_3^+ KER spectrum and anisotropy, β_2 values. $2hv = 67984 \text{ cm}^{-1}$.

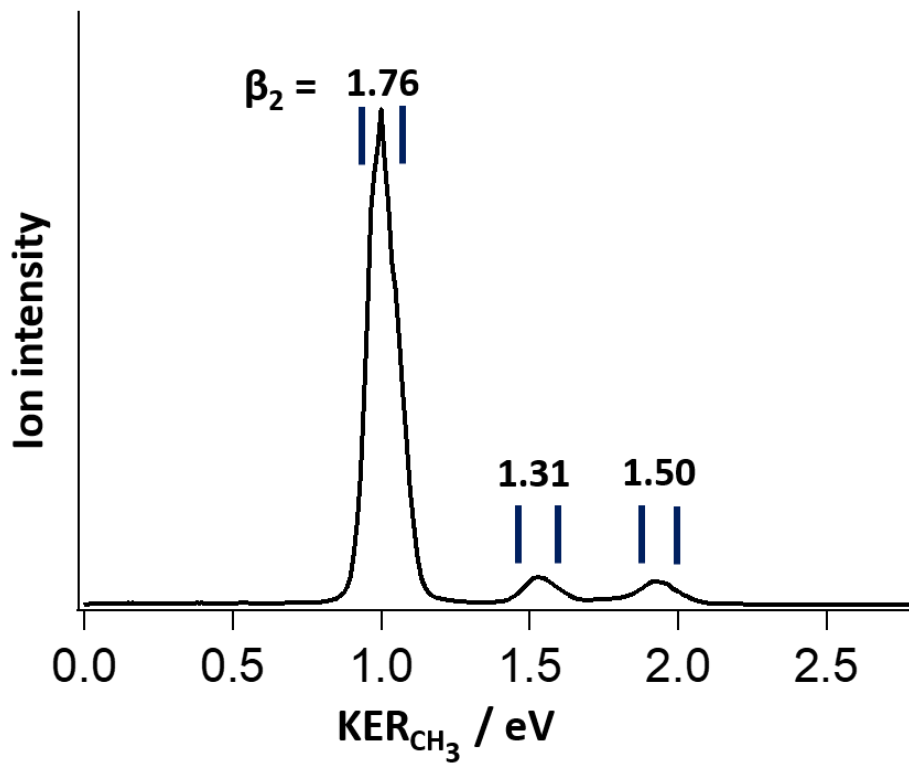


Fig. S4-h: CH_3^+ KER spectrum and anisotropy, β_2 values. $2hv = 69783 \text{ cm}^{-1}$.

Fig. S5.

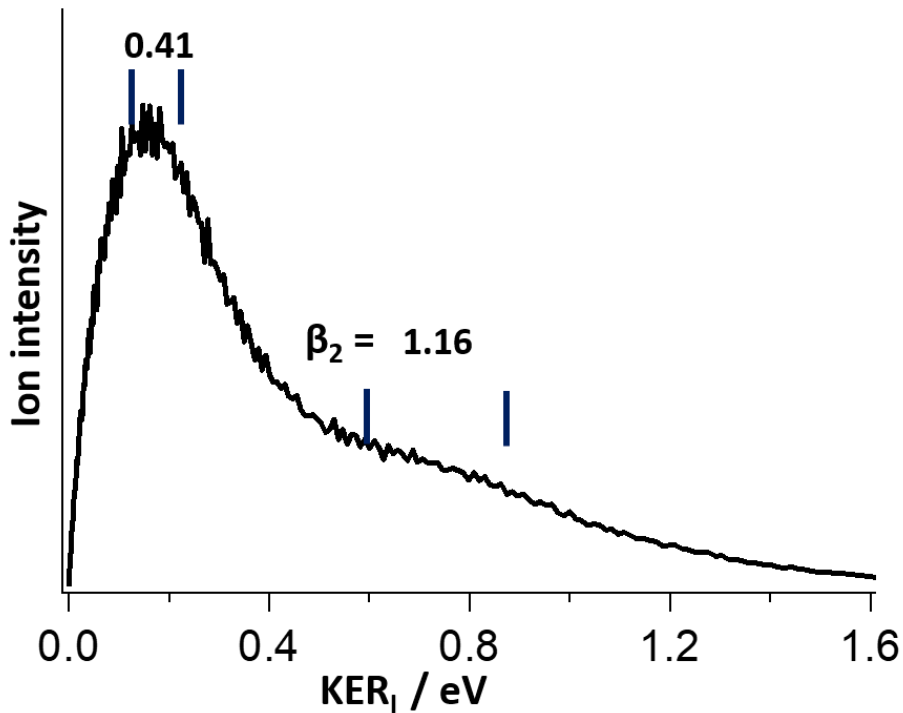


Fig. S5-a: I^+ KER spectrum and anisotropic β_2 values. $2hv = 55700 \text{ cm}^{-1}$.

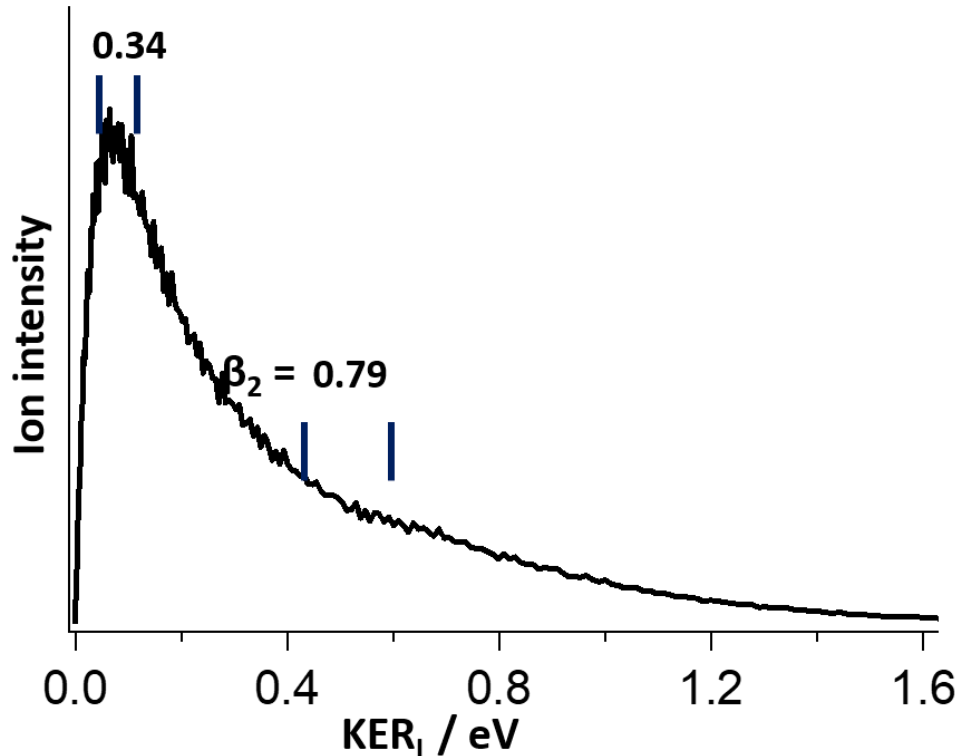


Fig. S5-b: I^+ KER spectrum and anisotropic β_2 values. $2hv = 58926 \text{ cm}^{-1}$.

Fig. S5.

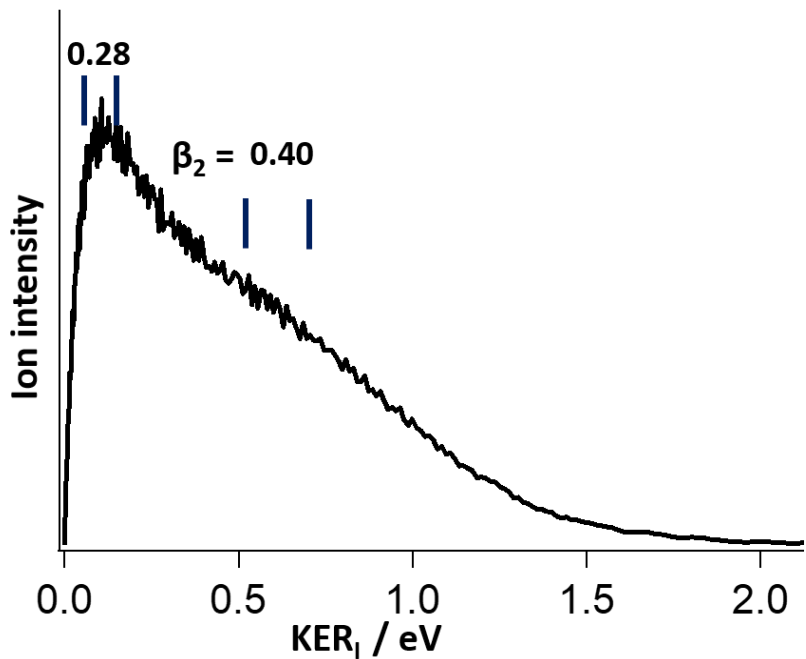


Fig. S5-c: I^+ KER spectrum and anisotropic β_2 values. $2hv = 59362 \text{ cm}^{-1}$.

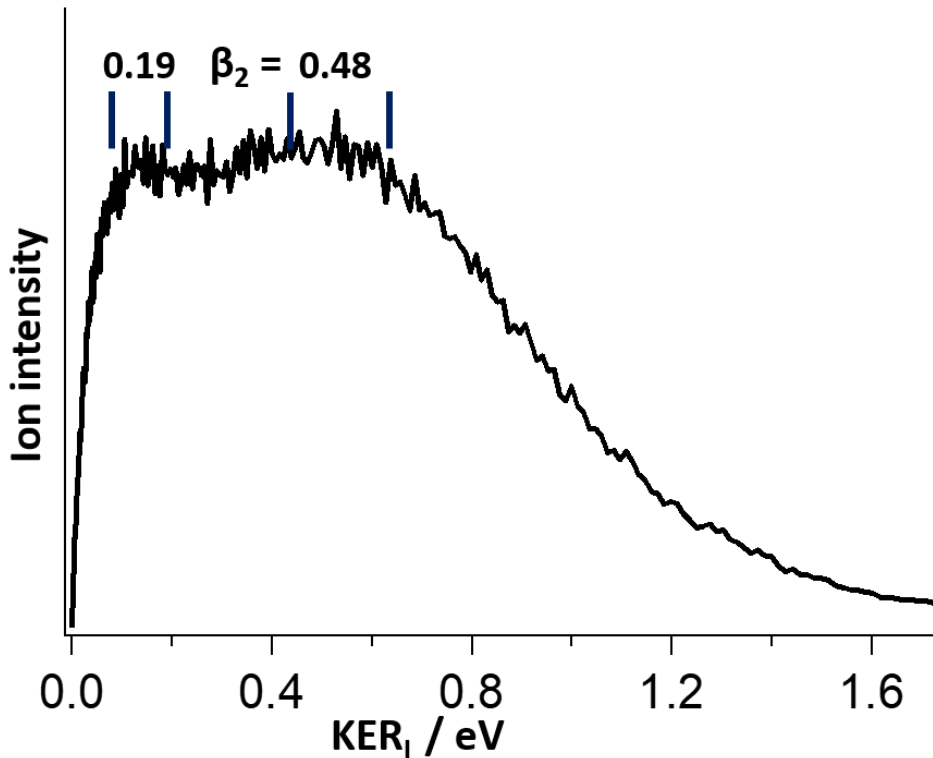


Fig. S5-d: I^+ KER spectrum and anisotropic β_2 values. $2hv = 61632 \text{ cm}^{-1}$.

Fig. S5.

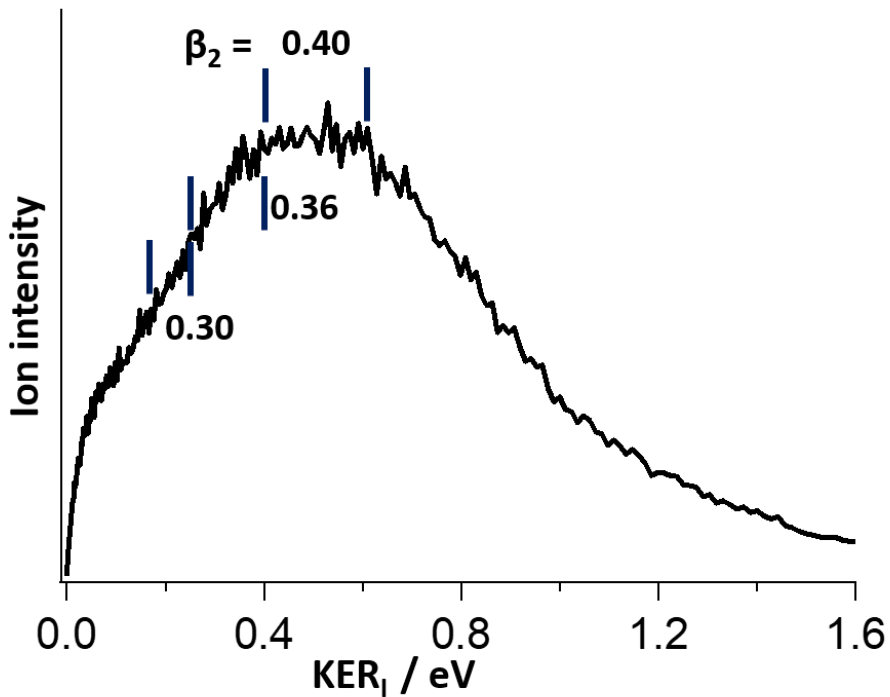


Fig. S5-e: I^+ KER spectrum and anisotropic β_2 values. $2hv = 63067 \text{ cm}^{-1}$.

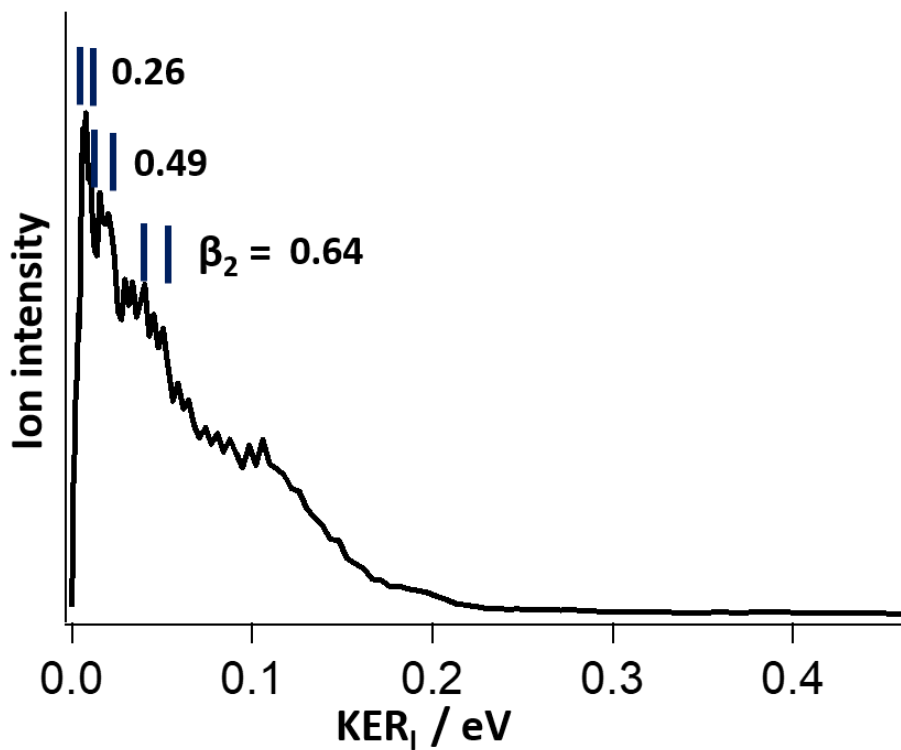


Fig. S5-f: I^+ KER spectrum and anisotropic β_2 values. $2hv = 64484 \text{ cm}^{-1}$.

Fig. S5.

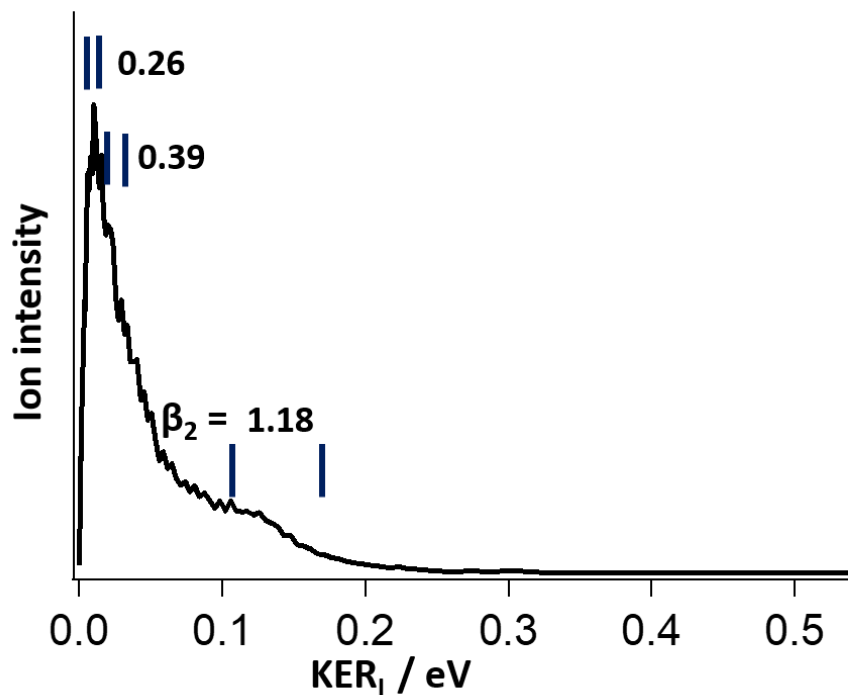


Fig. S5-g: I^+ KER spectrum and anisotropic β_2 values. $2hv = 67984 \text{ cm}^{-1}$.

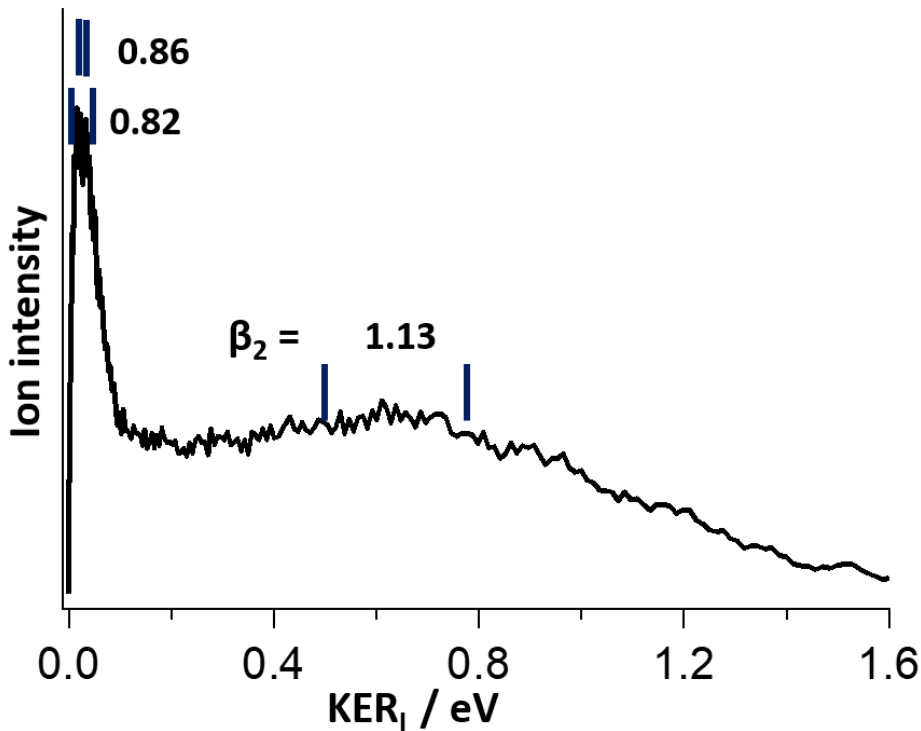


Fig. S5-h: I^+ KER spectrum and anisotropic β_2 values. $2hv = 69783 \text{ cm}^{-1}$.

Table.S1: Anisotropy parameters (β) from figures S4a-h (CH_3^+ images / KERs) and major fragmentation channels (see paper main text).

Figure	$2hv / cm^{-1}$	KER / eV	Major Channels	β_2	Δ	β_4	Δ	β_6	Δ
S3-a	55700	0.05–0.22	3c,4	0.77	± 0.01	-0.08	± 0.1	-0.01	± 0.01
		0.03–0.34		0.79	± 0.01	-0.08	± 0.1	-0.01	± 0.01
S3-b	58926	0.07–0.11	3c,4	0.33	± 0.01	0.07	± 0.01	-0.05	± 0.01
		0.13–0.23		0.43	± 0.01	-0.06	± 0.01	-0.04	± 0.01
S3-c	59362	0.07–0.11	3c,4	0.26	± 0.01	0.05	± 0.01	-0.07	± 0.02
		0.13–0.18		0.31	± 0.01	-0.06	± 0.01	0.01	± 0.01
		0.28–0.38		0.43	± 0.02	-0.07	± 0.02	-0.08	± 0.02
S3-d	61632	0.22–0.50	3b	0.55	± 0.04	0.1	± 0.05	-0.07	± 0.05
		0.79–0.95		0.90	± 0.06	0.04	± 0.07	-0.18	± 0.07
		1.13–1.69		0.91	± 0.12	0.08	± 0.13	-0.42	± 0.14
S3-e	63067	90–110	3b	0.70	± 0.05	-0.09	± 0.05	-0.12	± 0.06
		120–140		0.81	± 0.06	-0.13	± 0.07	-0.15	± 0.07
		150–170		0.98	± 0.09	-0.22	± 0.10	-0.14	± 0.10
S3-f	64484	120–140	3b	1.11	± 0.06	-0.03	± 0.05	-0.18	± 0.06
		140–160		1.05	± 0.09	-0.09	± 0.09	-0.08	± 0.10
		160–180		1.17	± 0.08	-0.02	± 0.08	-0.11	± 0.09
S3-g	67984	140–160	3b	1.13	± 0.02	-0.13	± 0.04	0.01	± 0.05
		130–170		1.12	± 0.02	-0.19	± 0.02	-0.00	± 0.03
S3-h	69783	0.93–1.03	1	1.76	± 0.06	-0.08	± 0.05	0.04	± 0.05
		1.43–1.55		1.31	± 0.23	-0.35	± 0.22	-0.16	± 0.23
		1.82–1.95		1.50	± 0.11	-0.18	± 0.10	-0.23	± 0.120

Table.S2: Anisotropy parameters (β) from figures S5a-h (I^+ images / KERs) and major fragmentation channels (see paper main text).

Figure	$2hv/cm^{-1}$	KER / eV	Major Channels	β_2	Δ	β_4	Δ	β_6	Δ
S5-a	55700	0.014–0.032	3c,4	0.86	± 0.01	-0.07	± 0.01	-0.03	± 0.01
		0.007–0.030		0.82	± 0.01	-0.11	± 0.01	-0.03	± 0.01
		0.504–0.788		1.13	± 0.03	0.03	± 0.04	0.00	± 0.04
S5-b	58926	0.007–0.014	3c,4	0.26	± 0.02	-0.02	± 0.00	-0.01	± 0.00
		0.014–0.027		0.39	± 0.01	-0.06	± 0.01	0.00	± 0.01
		0.106–0.148		1.18	± 0.06	-0.20	± 0.10	0.21	± 0.10
S5-c	59362	0.005–0.011	3c,4	0.26	± 0.00	-0.05	± 0.00	-0.00	± 0.00
		0.014–0.024		0.49	± 0.01	-0.06	± 0.01	0.03	± 0.01
		0.040–0.051		0.64	± 0.02	-0.12	± 0.02	0.09	± 0.02
S5-d	61632	0.172–0.284	3b	0.30	± 0.01	0.00	± 0.01	0.01	± 0.01
		0.284–0.424		0.36	± 0.01	0.00	± 0.02	0.01	± 0.02
		0.424–0.592		0.40	± 0.01	0.05	± 0.02	0.02	± 0.02
S5-e	63067	0.059–0.197	3b	0.19	± 0.01	0.03	± 0.01	0.02	± 0.01
		0.424–0.592		0.48	± 0.01	0.02	± 0.02	-0.01	± 0.02
S5-f	64484	0.065–0.130	3b	0.28	± 0.00	0.01	± 0.01	-0.01	± 0.01
		0.504–0.686		0.40	± 0.01	-0.01	± 0.01	0.02	± 0.01
S5-g	67984	0.043–0.106	3b	0.34	± 0.00	0.03	± 0.00	-0.01	± 0.00
		0.424–0.592		0.79	± 0.02	0.11	± 0.02	-0.01	± 0.02
S5-h	69783	0.139–0.187	1	0.41	± 0.00	0.02	± 0.00	0.00	± 0.00
		0.592–0.788		1.16	± 0.01	0.09	± 0.01	0.00	± 0.01